Food Research 6 (3) : 34 - 41 (June 2022)
Journal homepage: https://www.myfoodresearch.com

FOOD RESEARCH

FULL PAPER

Breadfruit (*Artocarpus altilis*) starch-based nanoparticle formation through dropwise mixing nanoprecipitation

[1]Harsanto, B.W., [1,*]Pranoto, Y., [1]Supriyanto and [2]Kartini, I.

[1]*Department of Food and Agricultural Product Technology, Faculty of Agricultural Technology, Universitas Gadjah Mada, Jl. Flora No.1, Yogyakarta 55281, Indonesia*
[2]*Department of Chemistry, Faculty of Mathematics and Natural Sciences, Universitas Gadjah Mada, Jl. Kaliurang KM. 5, Sekip Utara, Yogyakarta 55281, Indonesia*

Article history:
Received: 7 May 2021
Received in revised form: 16 June 2021
Accepted: 5 September 2021
Available Online: 8 May 2022

Keywords:
Breadfruit,
Starch nanoparticle,
Nanoprecipitation,
Mixing,
Surfactant

DOI:
https://doi.org/10.26656/fr.2017.6(3).308

Abstract

Starch nanoparticles from breadfruit (*Artocarpus altilis*) have been prepared using nanoprecipitation. The study aimed to investigate the performance of dropwise and direct mixing of ethanol as a non-solvent in the presence of and without surfactant (Tween 80) into breadfruit suspension during nanoprecipitation. The resulting breadfruit starch nanoparticles were evaluated for particle size and shape by particle size analysis, transmission electron microscopy (TEM), and scanning electron microscopy (SEM), crystal pattern by X-ray diffraction (XRD), and functional group by FTIR spectrophotometer. It was observed that performing the dropwise mixing technique without Tween 80 produced particles in the nanometer scale (175 nm), with uniform size distribution (18-459 nm), a porous surface, and an amorphous phase (single XRD peak at 19°). These breadfruit starch nanoparticles pave the way for incorporating starch products into a wide array of industry-application.

1. Introduction

Breadfruit (*Artocarpus altilis*) is a commodity widely available in Indonesia. A breadfruit tree can produce 250 fruits per year (Liu *et al*., 2014). However, breadfruit has a short shelf-life, with fruit deterioration 5 days after harvest (Worrell *et al*., 2002). Moreover, breadfruit processing is usually only boiled, steamed, or fried (short shelf life) (Sikarwar *et al*., 2014). On the other hand, breadfruit has soft tissue and high starch content, thus facilitating the starch extraction process (Adebayo *et al*., 2008). Several studies have reported that the starch content of breadfruit ranges from 15% to 20% (Adinugraha and Kartikawati, 2012; Sikarwar *et al*., 2014). Thus, breadfruit-based starch nanoparticles can be generated as stable, processed forms (Adebowale *et al*., 2005).

Starch from breadfruit was known to have a small granule size (<10 µm) (Tan *et al*., 2017) and medium amylose (20%) (Anwar *et al*., 2016), making it suitable for preparing nanoparticles. Qin *et al*. (2016) found that starch with small granule size and medium amylose had smaller and uniform nanoparticles than low or high amylose starch with large granule size. Hence, there is interest in producing starch nanoparticles from breadfruit.

Starch nanoparticles have the intrinsic characteristics of native starch, such as biodegradable, non-toxic, and biocompatible. In addition, they have a 100-200 nm size range, much smaller than the micrometre scale of native starch. Therefore, they have the advantage of having a high surface-to-volume ratio, making them suitable for a wide range of applications in foods (Liu *et al*., 2016), as well as in pharmaceuticals, for controlled drug release (Mahanta *et al*., 2019) and dentistry (Balhaddad *et al*., 2019). Furthermore, the small size of starch nanoparticles increases the adsorption capacity and decreases diffusion-related limitations. Sun (2018) explained that starch nanoparticles could overcome various limitations of native starch and can be used in the nanocomposite or emulsion field.

Nanoprecipitation is a method of making starch nanoparticles, usually called the solvent displacement method (Wu *et al*., 2016). The precipitation process includes the rapid diffusion of polymer solution (solvent) into the aqueous (non-solvent) phase or vice versa. Hence, a decrease in the interface tension of the two phases might occur, followed by nucleation-growth and leading to nanometer-scale colloid particles (de Oliveira *et al*., 2013; Chang *et al*., 2017). The advantages of using this method are the simplicity of the process (without

*Corresponding author.
Email: *pranoto@ugm.ac.id*

eISSN: 2550-2166
Published by Rynnye Lyan Resources

special equipment) and the ability to produce nanometer-scale particles homogeneously (Perevyazko *et al*., 2012; Joye and McClements, 2013). El-Sheikh (2017) reported that 62.5 nm of waxy maize starch nanoparticles could be formed through nanoprecipitation.

The process of mixing polymer (starch) and a non-solvent is a crucial stage in nanoprecipitation, which can induce the formation of particle nuclei (nucleation) and particle growth (Sun, 2018). The addition of surfactants is sometimes used to control particle growth. Therefore, the technique of mixing and surfactant presence becomes an essential aspect of nanoprecipitation. Several studies have investigated various mixing techniques (dropwise and direct mixing) (Saari *et al*., 2017) or the effect of surfactant (Hebeish *et al*., 2014) in the preparation of maize starch nanoparticles. However, no studies have addressed nanoparticles from breadfruit starch.

This study aimed to investigate the effect of the mixing technique and the surfactant addition on the characteristics of the breadfruit starch nanoparticles through the nanoprecipitation method. Ethanol was used as a non-solvent because of its non-toxic and high affinity with a starch solution (Wu *et al*., 2016). Meanwhile, a food-grade and hydrophilic surfactant, Tween 80, was used in this study. The particle size and shape, XRD pattern, and FTIR profile of the breadfruit starch nanoparticles were evaluated to determine the characteristics of the resulting breadfruit starch nanoparticles.

2. Materials and methods

2.1 Materials

Mature stage-breadfruit (hard texture on fruit flesh) was obtained from local farmers in Cilacap, Central Java, Indonesia. Chemical reagents, such as absolute ethanol (≥99% purity), Tween 80, and sodium hydroxide (NaOH), were purchased from Merck, Germany.

2.2 Extraction of breadfruit starch

Extraction of breadfruit starch (BS) was initially carried out by peeling of flesh fruit and washing. Then, the flesh fruit was soaked in $CaCO_3$-water solution (1% w/v), followed by adding excessive water to neutralize the alkaline-flesh fruit into a neutral condition (pH 7). In the neutral condition, the flesh fruit was blended with water in a milling instrument (Phillips HR2115, Phillips BV, Netherlands), resulting in a slurry. Next, the slurry was filtered using a cloth to obtain the filtrate and continued by settling the filtrate down for 18 hrs. The sediment was then sun-dried for 10 hrs, ground, and 150 mesh-sieved to obtain the BS powder. Then, the BS powder was tightly packed in LDPE plastic and then stored at ambient temperature for analysis. The powder was later used as a raw material to prepare breadfruit starch nanoparticles (BSN).

2.3 Preparation of breadfruit starch nanoparticles

Breadfruit starch nanoparticles (BSN) preparation was carried out through the nanoprecipitation method, according to El-Sheikh (2017). The BSN preparation was started with cold-NaOH gelatinization. Firstly, 5 g of BS, 1.5 g of NaOH, and 2.7 g of glycerol were vigorously mixed in 100 mL of distilled water at room temperature for 15 min using a homogenizer, resulting in BS suspension. Next, 100 mL of absolute ethanol was added to the BS suspension by either direct or dropwise mixing, thereby the precipitation occurs. Tween 80 (0.25% (v/v)) was also added to the starch solution-ethanol mixture. Next, stirring was continued for 15 mins using a homogenizer (Ultra-turrax Homogenizer T50 Basic, IKA, Germany) at 4000 rpm. The starch precipitate was obtained after centrifugation at 4000 rpm, room temperature and washing with ethanol-distilled water (80:20) mixture. The starch precipitate was then dried using a cabinet drier at 60^{o}C overnight. Finally, the dried BSN was ground and 150 mesh-sieved to obtain the BSN powder. A BSN preparation without the addition of Tween 80 was also carried out for comparison.

2.4 Characterization of breadfruit starch and breadfruit starch nanoparticles

In the early stages, BS was characterized by proximate analysis, according to AOAC (2005), i.e., moisture content using the thermo-gravimetric method, lipid content using the Soxhlet method, ash content, and protein content using the Kjeldahl method. The next stage depicts the BS particle size and shape were compared with the BSN to investigate the alteration during nanoprecipitation. The XRD pattern and FTIR profile of BS and BSN were also evaluated.

2.4.1 Particle size

The BS and BSN particle sizes were determined using a Particle Size Analyzer LA-960 (Horiba, Japan) and Malvern Zetasizer Nano ZSP (Malvern Instruments Ltd., UK.) for the size of >1000 nm (static laser scattering) and ≤1000 nm (dynamic laser scattering), respectively. The powder sample was diluted in deionized water (0.1 mg/ml) before measurement.

2.4.2 Particle shape

The BS and BSN particles were observed using a Scanning Electron Microscope JSM-6510LA (JEOL, Japan). The powder was placed into a stub specimen and coated with a gold layer.

The particle shape was also observed with transmission electron microscopy (TEM) (JEOL JEM-1400, JEOL, USA). The drop of sample dispersion (starch nanoparticle in deionized water) was placed on an amorphous carbon film-coated copper grid (400 mesh).

2.4.3 X-Ray Diffraction (XRD) analysis

The crystal patterns of BS and BSN were observed using an X-ray Diffractometer (D2 Bruker, Germany) with a wavelength of 1,542 Å at 40 kV and 250 mA. The scanning range was 5°-70°, with a scan speed of 15°/min and a step width of 0.5 sec/step.

2.4.4 Fourier Transform InfraRed (FTIR) analysis

The functional groups of BS and BSN were analyzed using Fourier Transform Infrared (FTIR) (Shimadzu, Japan) with a 400 - 4000 cm^{-1} scanning range set. The pellet sample was produced by mixing 1 mg of the sample with 200 mg potassium bromide (KBr).

2.5 Statistical analysis

Experiments were carried out through a completely randomized design with two replications. Data were then analyzed using statistical software, SPSS v.25 (SPSS inc., USA), with the One-way ANOVA method. The significance between treatments was evaluated according to Duncan's test at $\alpha = 5\%$ ($p \leq 0.05$).

3. Results and discussion

3.1 Proximate composition of breadfruit starch (BS)

In this study, the BS was extracted through the wet milling method. The obtained BS powder was white, with a moisture content of 11.98% (Table 1), similar to Anwar *et al*. (2016) report. Commercial starch usually has a moisture content of about 12% (Ledezma, 2018). Meanwhile, another study found that breadfruit starch approximately contained a moisture content of 13% (Tan *et al*., 2017).

Table 1. Proximate content of breadfruit starch

Parameter	Value (%)
Moisture content	11.98±0.10
Ash content	0.72±0.14
Lipid content	0.75±0.04
Protein content	1.76±0.21
Carbohydrate content[a]	84.79±0.01

[a]Value was determined based on calculation as: 100% - (moisture content + ash content + lipid content + protein content). Values are presented as mean±SD.

Adebowale *et al*. (2005) reported similar results for their BS (water content: 13.05%; ash content: 0.35%; protein content: 1.61%; fat content: 0.51%; carbohydrate content: 84.48%). The ash content of starch represents the minor amount of minerals in starch (<0.5%). Inorganic minerals may come from a phosphate portion naturally contained in starch (Nwokocha and Williams, 2011). Phosphorus can exist as phosphate monoester or phospholipid (Alcazar-Alay and Meireles, 2015). Meanwhile, starch protein content usually comes from the enzyme residues used in starch synthesis, particularly starch synthase (Tester *et al*., 2004). Enzyme residues can indeed be detected as proteins in the Kjeldahl analysis method because they contain amino acids that makeup proteins containing N atoms.

3.2 Particle size

The BS showed unimodal particle size distribution of about 10 µm (Figures 1A and 1B). Other studies also found that the size of BS ranged from 2.25 to 8.42 µm (<10 µm) (Nwokocha and Williams, 2011; Tan *et al*., 2017). Wang *et al*. (2011) found 87% of breadfruit starch granules with a diameter of 4 -16 µm (mean: 10 µm), which indicates the small size of breadfruit starch granules.

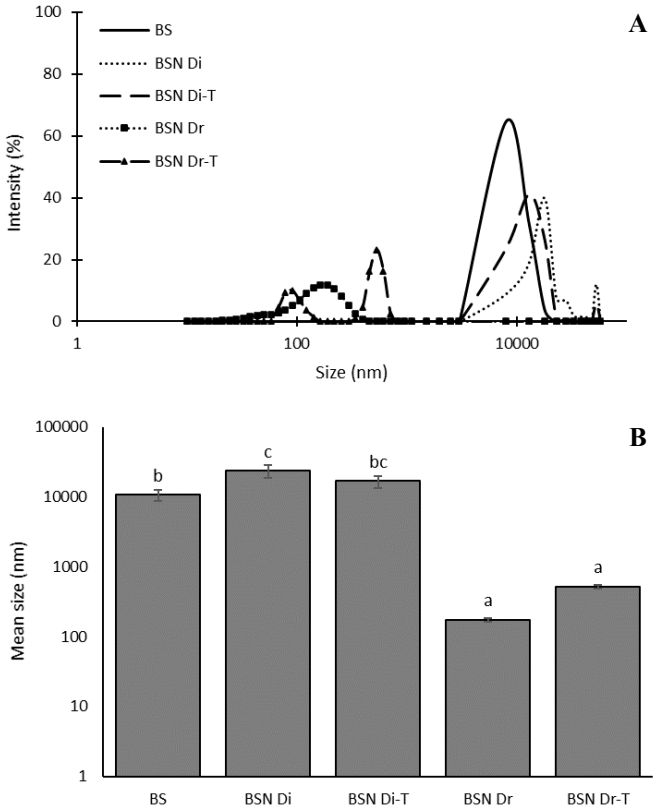

Figure 1. A) Particle size distribution and B) mean of particle size of BS (breadfruit starch), BSN Di (direct mixing without Tween 80), BSN Di-T (direct mixing with Tween 80), BSN Dr (dropwise mixing without Tween 80), BSN Dr-T (dropwise mixing with Tween 80). Bars with different letter notations are significantly different among treatments ($p \leq 0.05$).

Firstly, the nanoprecipitation was performed by direct mixing treatment with and without Tween 80. The surfactant is supposed to retain the nanoparticle starch from agglomeration. It is observed that the particle size

distribution of the resulted starches (BSN Di and BSN Di -T) was greater than that of the BS, with or without the addition of Tween 80 (Figure 1A). The precipitation is thought to be so fast, therefore the nanoparticle formation could not be controlled very well. Large aggregates seem to be spontaneously formed resulting in mean particle size of 17-23 µm. It is noted that the surfactant involved reaction formed a slightly smaller particle as expected. Therefore, for the subsequent treatment, dropwise mixing was introduced. Slow and controlled precipitation under agitation is expected to obtain nanometer-scale breadfruit starch.

Figure 1B has shown that the dropwise mixing could shift the particle size distribution of the BS into a smaller particle size (<1000 nm) with a mean particle size of 175 nm for BSN Dr and 520 nm for BSN Dr-T. The large particles detected in the particle size distribution curve of BSN Dr-T were assumed to result in an aggregate of small nanoparticles formed during centrifugation and washing (Sadeghi *et al*., 2017).

It is seen that the application of dropwise mixing gave a smaller mean particle size (<600 nm) than direct mixing (>16000 nm) ($p \leq 0.05$) (Figure 1B). Saari *et al*. (2017) reported that the direct mixing of ethanol into a waxy maize starch solution produced more particles of the small fraction (71%) than dropwise mixing (65-66%). These different results were probably due to differences in starch sources and starch solvents. In addition, the molecular state of the breadfruit starch polymer was not in the ideal dispersed state, ensuring the separation into nano-domains following the addition of ethanol.

The addition of Tween 80 resulted in a wider size distribution than that without Tween 80 when dropwise mixing was applied (Figure 1A). Cao (2004) explained that nuclei compounds formed simultaneously would have the same growth conditions to form uniform nanoparticles. These results indicate that the presence of Tween 80 might reduce the uniformity of growth conditions of nuclei. Meanwhile, the use of ten drops of Tween 80 was assumed to exceed the critical micelle concentration (CMC) of Tween 80, therefore the aggregates (micelle) were formed in solution (Szymczyk and Taraba, 2017) and detected as large particles.

In the dropwise mixing treatment, Tween 80 made the mean particle size larger than without Tween 80 (Figure 1B). The addition of Tween 80 was believed to cause an excessive amount of free emulsifier molecules to the particles and result in larger particle size (Hebeish *et al*., 2014). These results were different from those of other studies, where the addition of Tween 80 could produce particles of between 60-150 nm (Hebeish *et al*., 2014; El-Sheikh, 2017). This difference was possibly due to differences in starch sources, the concentration of Tween 80 added, and the particles drying conditions. The large particle size could be related to the less effective direct mixing technique of ethanol into breadfruit starch solution compared to the dropwise technique.

3.3 Particle shape

Particle shape observations were carried out using SEM and TEM. Electrons with energies of hundreds of eV to 50 eV (SEM) and 100 keV to 1 MeV (TEM) contribute to observing the surface and internal parts of the specimen (Cao, 2004).

BS was a solid sphere and slightly clustered (Figure 2). The shape of the BS in other studies was also sub-spherical (small round) and clustered (Adebayo *et al*., 2008; Nwokocha and Williams., 2011). During the preparation of starch nanoparticles, there was a change in the particles' shape into irregular and aggregated shapes (Figure 2A), although they appeared smaller by TEM observation (Figure 2B). The cold-NaOH gelatinization of starch might be responsible for the irregular shaped BSN.

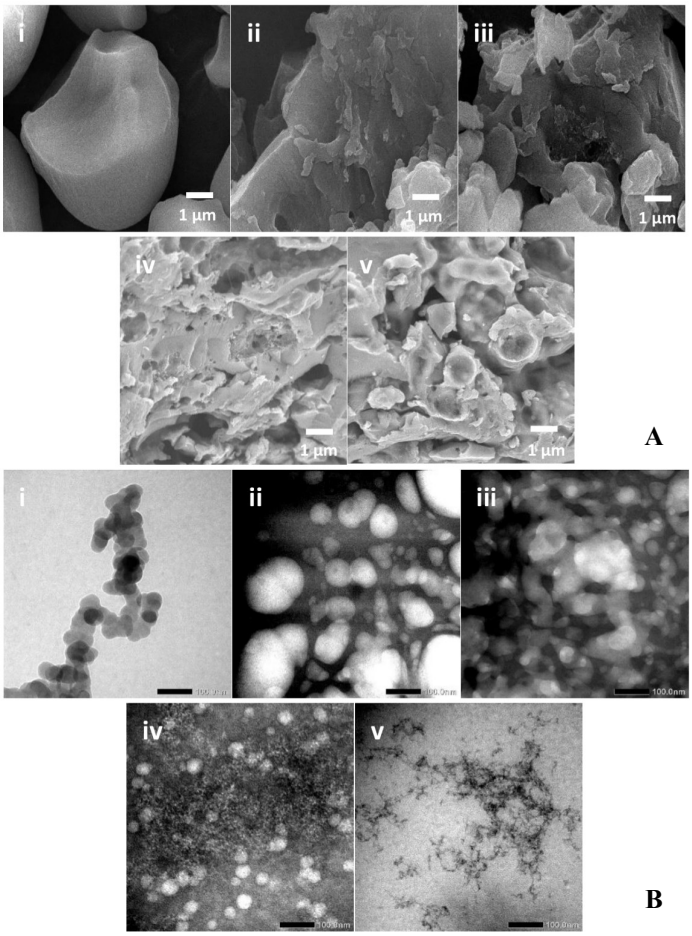

Figure 2. SEM image at 10,000× magnification (scale bar: 1 µm) (A) and TEM image (scale bar: 100 nm) (B) of i) BS (breadfruit starch), ii) BSN Di (direct mixing without Tween 80), iii) BSN Di-T (direct mixing with Tween 80), iv) BSN Dr (dropwise mixing without Tween 80), v) BSN Dr-T (dropwise mixing with Tween 80).

The dropwise mixing technique provided a more porous surface in SEM observations than direct mixing, either with or without Tween 80 (Figure 2A). Meanwhile, the particles appeared smaller in dropwise mixing than in direct mixing when observed with TEM (Figure 2B). Ethanol would react more regularly when mixed slowly in the starch solution. Therefore, dropwise mixing could result in more effective mixing than direct mixing, which could be attributed to the formation of nanoscale and porous particles.

Interestingly, dropwise mixing followed by adding Tween 80 resulted in tiny particles aggregated intensively (TEM observation) (Figure 2B). Thus, aggregates could indeed be formed from the formation of complexes between surfactants and starches. Theoretically, non-ionic surfactants will bind first with amylose and then proceed to amylopectin (Ledezma, 2018). Richardson *et al*. (2004) stated that amylose could form spherical aggregates in the presence of surfactants.

3.4 X-ray diffraction pattern

BS had diffraction peaks at 5.8°, 11°, 13°, 15°, 17°, 19°, 22°, and 24° (Figure 3), which showed a B-type crystal pattern, as described previously (Nwokocha and Williams, 2011, Tan *et al*., 2017). Meanwhile, all BSN samples had only one diffraction peak at 19° (Figure 3). The loss of diffraction peaks occurred due to structural damage to the semi-crystalline structure (Tan *et al*., 2017).

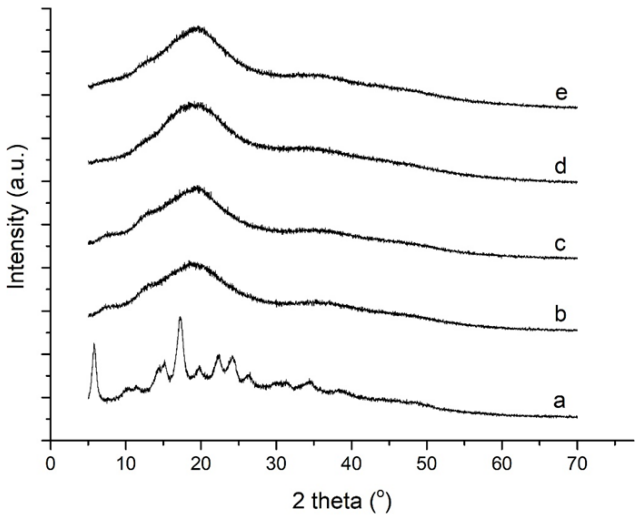

Figure 3. XRD pattern of a) BS (breadfruit starch), b) BSN Di (direct mixing without Tween 80), c) BSN Di-T (direct mixing with Tween 80), d) BSN Dr (dropwise mixing without Tween 80), e) BSN Dr-T (dropwise mixing with Tween 80).

These findings suggest that BSN had a V-type crystalline pattern, which was likely derived from the complex between amylose and ethanol. During nanoprecipitation, ethanol reacts with the starch suspension to form a single helix complex (Qin *et al*., 2016). Amylose complexes are generally insoluble helix with different crystalline characteristics from the A crystal pattern and the B crystal pattern (Copeland *et al*., 2009). Other researchers also reported starch nanoparticles with V-type crystals (Hebeish *et al*., 2014; El-Sheikh, 2017).

The addition of Tween 80 produced an XRD pattern that was similar to without the addition of Tween 80, either by dropwise or direct mixing (Figure 3). The surfactant addition to starch might be related to the formation of inclusion complexes between amylose and surfactants (Ledezma. 2018). Thus, the peak diffraction at 19° in BSN might arise from the presence of an amylose-ethanol complex or an amylose-surfactant complex.

Overall, BS was semi-crystalline, and BSN was amorphous. The cold-NaOH gelatinization can break the bonds inside the crystalline region of starch (Larsen *et al*., 2013). Moreover, dissolving starch molecules in NaOH solution followed by precipitation causes damage to the crystalline structure of amylopectin. As a result, the nanoparticle character becomes amorphous (Hebeish *et al*., 2014).

3.5 Fourier Transform InfraRed (FTIR) profile

BS had an FTIR profile similar to that of BSN, with peaks at 3400-3500 cm^{-1} and 2900 cm^{-1} (Figure 4). This profile indicates that BS and BSN have O-H bonds stretching vibrations from the OH group on glucose units (showing inter-and intra-molecular bonds of starch). The C-H stretching bonds (2900 cm^{-1}) from methylene were also present (Shi *et al*., 2012, Li *et al*., 2016), relating to C-H bonds in BS and BSN.

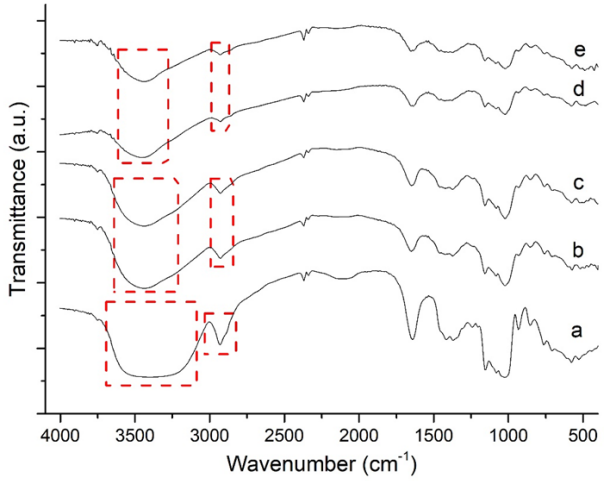

Figure 4. FTIR profiles a) BS (breadfruit starch), b) BSN Di (direct mixing without Tween 80), c) BSN Di-T (direct mixing with Tween 80), d) BSN Dr (dropwise mixing without Tween 80), e) BSN Dr-T (dropwise mixing with Tween 80). The red dotted box showed the difference in intensity of the spectra at 3400-3500 cm^{-1} and 2900 cm^{-1} between BS (a), BSN with direct mixing (b,c), and BSN with dropwise mixing (d,e).

El-Sheikh (2017) mentioned that the FTIR peaks between native starch and starch nanoparticles are mostly similar in their position, but there was a slight increase/decrease in intensity. This similarity indicated no significant change in chemical structure when native starch was processed into starch nanoparticles. As seen in Figure 4, the peak area for BSN was lower than for BS, either at 3400-3500 cm^{-1} or 2900 cm^{-1}. This result was due to the cutting of α-1.4 glycosidic bonds during starch gelatinization (Koh and Long, 2012), e.g., cold-NaOH gelatinization, decreasing the number of OH and CH bonds. Another study also stated that OH stretching intensity from starch nanoparticles was lower than that of native starch (positions around 3405 and 3416 cm^{-1}) (El-Sheikh, 2017).

The choice of mixing technique and the presence of Tween 80 did not have a significant impact on the FTIR profile of BSN. The similarity of FTIR profiles was also reported by Hebeish *et al*. (2014), who compared starch nanoparticles with Tween 80 and without Tween 80. When added, Tween 80 was thought to contribute to the presence of FTIR peaks at positions 3468 and 1639 cm^{-1} (O-H bond), 2855 cm^{-1} (C-H bond), 1732 cm^{-1} (C=O bond), and 1092 cm^{-1} (C-O-C bond) (Khan *et al*., 2010).

4. Conclusion

Breadfruit starch can be used as an appropriate raw material in nanoparticle preparation. Overall, the mixing technique and adding surfactants affect the characteristics of the breadfruit starch nanoparticles produced by the nanoprecipitation method. The performance of dropwise mixing without Tween 80 was an effective approach to producing nanometer-sized starch particles (<200 nm) with a uniform size distribution, porous surface, and an amorphous phase. Therefore, breadfruit starch nanoparticles can be widely applied in the industry field to increase the value of processed breadfruit.

Conflict of interest

The authors declare no conflict of interest.

Acknowledgements

The study was funded by Ministry of Research, Technology, and Higher Education in Indonesia through funding scheme of *Pendidikan Magister Menuju Doktor untuk Sarjana Unggul* (PMDSU) with contract number 2977/UN1.DITLIT/DIT-LIT/LT/2019.

References

Adebayo, S.A., Brown-Myrie, E. and Itiola, O.A. (2008). Comparative disintegrant activities of breadfruit starch and official corn starch. *Powder Technology*, 181(2), 98–103. https://doi.org/10.1016/j.powtec.2006.12.013

Adebowale, K.O., Olu-Owolabi, B.I., Olawumi, E.K. and Lawal, O.S. (2005). Functional properties of native, physically and chemically modified breadfruit (*Artocarpus artilis*) starch. *Industrial Crops and Products*, 21(3), 343–351. https://doi.org/10.1016/j.indcrop.2004.05.002

Adinugraha, H.A. and Kartikawati, N.K. (2012). Variasi Morfologi dan Kandungan Gizi Buah Sukun. *Wana Benih*, 13(2), 99–106. [In Bahasa Indonesia].

Alcazar-Alay, S.C. and Meireles, M.A.A. (2015). Physicochemical properties, modifications and applications of starches from different botanical sources. *Food Science and Technology*, 35(2), 215-236. https://doi.org/10.1590/1678-457X.6749

Anwar, S.H., Rahmah, M., Safriani, N., Hasni, D., Rohaya, S. and Winarti, C. (2016). Exploration of breadfruit, jicama, and rice starches as stabilizer in food emulsion. *International Journal on Advanced Science Engineering Information Technology*, 6(2), 141-145. https://doi.org/10.18517/ijaseit.6.2.613

AOAC. (2005). Official Methods of Analysis. 18th ed. Maryland, USA: Association of Official Analytical Chemist International.

Balhaddad, A.A., Kansara, A.A., Hidan, D., Weir, M.D., Xu, H.H.K. and Melo, M.A.S. (2019). Toward dental caries: Exploring nanoparticle-based platforms and calcium phosphate compounds for dental restorative materials. *Bioactive Materials*, 4(1), 43–55. https://doi.org/10.1016/j.bioactmat.2018.12.002

Cao, G. (2004). Nanostructure and Nanomaterials: Synthesis, properties, and applications. London, United Kingdom: Imperial College Press. https://doi.org/10.1142/p305

Chang, Y., Yan, X., Wang, Q., Ren, L., Tong, J. and Zhou, J. (2017). High efficiency and low-cost preparation of size-controlled starch nanoparticles through ultrasonic treatment and precipitation. *Food Chemistry*, 227, 369–375. https://doi.org/10.1016/j.foodchem.2017.01.111

Copeland, L., Blazek, J., Salman, H. and Tang, M.C. (2009). Form and Functionality of Starch. *Food Hydrocolloids,* 23(6), 1527–1534. https://doi.org/10.1016/j.foodhyd.2008.09.016

de Oliveira, A.M., Jager, E., Jager, A., Stepanek, P. and Giacomelli, F.C. (2013). Physicochemical aspects behind the size of biodegradable polymeric nanoparticles: A step forward. *Colloids and Surfaces A: Physicochemical and Engineering Aspects*, 436,

1092–1102. https://doi.org/10.1016/j.colsurfa.2013.08.056

El-Sheikh, M.A. (2017). New technique in starch nanoparticles synthesis. *Carbohydrate Polymers*, 176, 214–219. https://doi.org/10.1016/j.carbpol.2017.08.033

Hebeish, A. El-Rafie, M.H., El-Sheikh, M.A. and Naggar, M.E. (2014). Ultra-fine characteristics of starch nanoparticles prepared using native starch with and without surfactant. *Journal of Inorganic and Organometallic Polymers and Materials*, 24(3), 515–524. https://doi.org/10.1007/s10904-013-0004-x

Joye, I.J. and McClements, D.J. (2013). Production of nanoparticles by anti-solvent precipitation for use in food systems. *Trends Food Science and Technology*, 34(2), 109–123. https://doi.org/10.1016/j.tifs.2013.10.002

Khan, Y., Durrani, S.K., Mehmood, M., Ahmad, J., Khan, M.R. and Firdous, S. (2010). Low Temperature Synthesis of Fluorescent ZnO Nanoparticles. *Applied Surface Science*, 257(5), 1756–1761. https://doi.org/10.1016/j.apsusc.2010.09.011

Koh, S.P. and Long, K. (2012). Comparison of physical, chemical and functional properties of broken rice and breadfruit starches against cassava starch. *Journal of Tropical Agriculture and Food Science*, 40(2), 211–219.

Larsen, F.H., Kasprzak, M.M., Laerke, H.N., Knudsen, K.E.B., Pedersen, S., Jorgensen, A.S. and Blennow, A. (2013). Hydration properties and phosphorous speciation in native, gelatinized and enzymatically modified potato starch analyzed by solid-state MAS NMR. *Carbohydrate Polymers*, 97(2), 502–511. https://doi.org/10.1016/j.carbpol.2013.05.014

Ledezma, C.C.Q. (2018). Starch in Food: Structure, function, and applications. 2nd ed. In Sjoo, M. and Nilsson, L. (Eds). Starch Interactions with Native and Added Food Components, p. 769-801. Duxford, United Kingdom: Woodhead Publishing. https://doi.org/10.1016/B978-0-08-100868-3.00020-2

Li, X., Qin, Y., Liu, C., Jiang, S., Xiong, L. and Sun, Q. (2016). Size-controlled starch nanoparticles prepared by self-assembly with different green surfactant: The effect of electrostatic repulsion or steric hindrance. *Food Chemistry*, 199, 356–363. https://doi.org/10.1016/j.foodchem.2015.12.037

Liu, Y., Maxwell, A., Jones, P., Muroh, S.J. and Ragone, D. (2014). Crop productivity, yield and seasonality of breadfruit (*Artocarpus* spp., Moraceae). *Fruits*, 69 (5), 345–361. https://doi.org/10.1051/fruits/2014023

Liu, C. Qin, Y., Li, XJ, Sun, Q.J., Xiong, L. and Liu, Z.Z. (2016). Preparation and characterization of starch nanoparticles via self-assembly at moderate temperature. *International Journal of Biological Macromolecules*, 84, 354–360. https://doi.org/10.1016/j.ijbiomac.2015.12.040

Mahanta, A.K., Senapati, S., Paliwal, P., Krishnamurthy, S., Hemalatha, S. and Maiti, P. (2019). Nanoparticle-Induced Controlled Drug Delivery Using Chitosan-Based Hydrogel and Scaffffold: Application to Bone Regeneration. *Molecular Pharmaceuitcs*, 16(1), 327–338. https://doi.org/10.1021/acs.molpharmaceut.8b00995

Nwokocha, L.M. and Williams, P.A. (2011). Comparative study of physicochemical properties of breadfruit (*Artocarpus altilis*) and white yam starches. *Carbohydrate Polymers*, 85(2), 294–302. https://doi.org/10.1016/j.carbpol.2011.01.050

Perevyazko, I.Y., Vollrath, A., Pietsch, C., Schubert, S., Pavlov, G.M. and Schubert, U.S. (2012). Nanoprecipitation of poly (methyl methacrylate)-based nanoparticles: Effect of the molar mass and polymer behavior. *Journal of Polymer Science Part A: Polymer Chemistry*, 50(14), 2906–2913. https://doi.org/10.1002/pola.26071

Qin, Y., Liu, C., Jiang, S., Xiong L. and Sun, Q. (2016). Characterization of starch nanoparticles prepared by nanoprecipitation: Influence of amylose content and starch type. *Industrial Crops and Products*, 87, 182-190. https://doi.org/10.1016/j.indcrop.2016.04.038

Richardson, G., Kidman, S., Langton, M. and Hermansson, A-M. (2004). Differences in amylose aggregation and starch gel formation with emulsifiers. *Carbohydrate Polymers*, 58(1), 7-13. https://doi.org/10.1016/j.carbpol.2004.06.013

Saari, H. Fuentes, C., Sjoo, M., Rayner, M. and Wahlgren, M. (2017). Production of starch nanoparticles by dissolution and non-solvent precipitation for use in food-grade Pickering emulsions. *Carbohydrate Polymers*, 157, 558–566. https://doi.org/10.1016/j.carbpol.2016.10.003

Sadeghi, R. Daniella, Z., Uzun, S. and Kokini, J. (2017). Effects of starch composition and type of non-solvent on the formation of starch nanoparticles and improvement of curcumin stability in aqueous media. *Journal of Cereal Science*, 76(6), 122–130. https://doi.org/10.1016/j.jcs.2017.05.020

Shi, A.M., Wang, L.J., Li, D. and Adhikari, B. (2012). The effect of annealing and cryoprotectants on the properties of vacuum-freeze dried starch nanoparticles. *Carbohydrate Polymers*, 88(4), 1334-1341. https://doi.org/10.1016/j.carbpol.2012.02.013

Sikarwar, M.S., Hui, B.J., Subramaniam, K., Valeisamy,

B.D., Yean, L.K. and Balaji, K. (2014). A Review on *Artocarpus altilis* (Parkinson) Fosberg (breadfruit). *Journal of Applied Pharmaceutical Science*, 4(8), 91 -97. https://doi.org/10.5530/fra.2014.2.7

Sun, Q. (2018). Starch in Food: Structure, function, and applications 2nd edition. In Sjoo, M. and Nilsson, L. (Eds). Starch Nanoparticle, p. 691-745. Duxford, United Kingdom: Woodhead Publishing. https://doi.org/10.1016/B978-0-08-100868-3.00018-4

Szymczyk, K. and Taraba, A. (2017). Properties of aqueous solutions of non-ionic surfactants, Triton X-114 and Tween 80, at temperatures from 293 to 318 K: Spectroscopic and ultrasonic studies. *Chemical Physics*, 483–484, 96–102. https://doi.org/10.1016/j.chemphys.2016.11.015

Tan, X., Li, X., Chen, L., Xie, F., Li, L. and Huang, J. (2017). Effect of heat-moisture treatment on multi-scale structures and physicochemical properties of breadfruit starch. *Carbohydrate Polymers*, 161, 286–294. https://doi.org/10.1016/j.carbpol.2017.01.029

Tester, R.F., Karkalas, J. and Qi, X. (2004). Starch—composition, fine structure and architecture. *Journal of Cereal Science*, 39(2), 151–165. https://doi.org/10.1016/j.jcs.2003.12.001

Wang, X., Chen, L., Li, X., Xie, F., Liu, H. and Yu, L. (2011). Thermal and rheological properties of breadfruit starch. *Journal of Food Science*, 76(1), E55-E61. https://doi.org/10.1111/j.1750-3841.2010.01888.x

Worrell, D.B., Carrington, C.S. and Huber, D.J. (2002). The use of low temperature and coatings to maintain storage quality of breadfruit, *Artocarpus altilis* (Parks.) Fosb. *Postharvest Biology and Technology,* 25(1), 33-40. https://doi.org/10.1016/S0925-5214(01)00143-0

Wu, X., Chang, Y., Fu, Y., Ren, L., Tong, J. and Zhou, J. (2016). Effects of non-solvent and starch solution on formation of starch nanoparticles by nanoprecipitation. *Starch/Staerke*, 68(3–4), 258–263. https://doi.org/10.1002/star.201500269

